Biomineralization of uranium-phosphates fueled by microbial 1 degradation of isosaccharinic acid (ISA)

Kuippers, G.; Morris, K.; Townsend, L. T.; Bots, P.; Kvashnina, K.; Bryan, N.; Lloyd, J. R.;

Originally published:

March 2021

Environmental Science & Technology 55(2021)8, 4597-4606

DOI: https://doi.org/10.1021/acs.est.0c03594

Biomineralization of uranium-phosphates fueled by microbial degradation of isosaccharinic acid (ISA)

Gina Kuippers[‡], Katherine Morris[‡], Luke T. Townsend[‡], Pieter Bots[‡,§], Kristina Kvashnina[⊥,†], Nicholas Bryan[#], Jonathan R. Lloyd[‡*]

[‡]Research Centre for Radwaste Disposal & Williamson Research Centre for Molecular Environmental Science, Department of Earth and Environmental Sciences, University of Manchester, Oxford Road, Manchester M13 9PL, UK

[§]Civil and Environmental Engineering, University of Strathclyde, Glasgow, UK

[#]National Nuclear Laboratory Limited, Chadwick House, Warrington Road, Birchwood Park, Warrington, WA3 6AE, UK

[⊥]The Rossendorf Beamline at ESRF-The European Synchrotron, CS40220, 38043 Grenoble Cedex 9, France

[†]Helmholtz Zentrum Dresden-Rossendorf (HZDR), Institute of Resource Ecology, P.O. Box 510119, 01314 Dresden, Germany

*Corresponding author e-mail: Jon.lloyd@manchester.ac.uk

Key words: Isosaccharinic acid, biodegradation, ningyoite, uranyl-phosphate, autunite, nuclear waste management

Abstract

Geological disposal is the preferred long-term solution for higher activity radioactive wastes (HAW) including Intermediate Level Waste (ILW). In a cementitious disposal system, cellulosic waste items present in ILW could undergo alkaline hydrolysis, producing significant quantities of isosaccharinic acid (ISA), a chelating agent for radionuclides. Although microbial degradation of ISA has been demonstrated, its impact upon the fate of radionuclides in a GDF is a topic of ongoing research. This study investigates the fate of U(VI) in pH neutral, anoxic, microbial enrichment cultures, approaching conditions similar to the far field of a GDF, containing ISA as the sole carbon source, and elevated phosphate concentrations, incubated both (i) under fermentation and (ii) Fe(III)-reducing conditions. In the fermentation experiment, U(VI) was precipitated as insoluble U(VI)-phosphates, whereas under Fe(III)-reducing conditions, the majority of the uranium was precipitated as reduced U(IV)-phosphates, potentially via

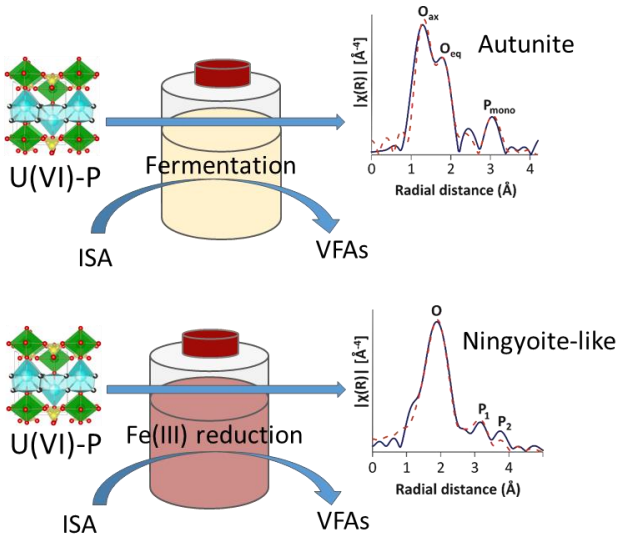

enzymatic reduction (mediated by metal-reducing bacteria including *Geobacter* species detected by 16S rRNA gene sequencing). Overall, this suggests the potential for the establishment of a microbially-mediated "bio-barrier" extending into the far field geosphere surrounding a GDF which has the potential to evolve in response to aspects of a GDF and can have a controlling impact on the fate of radionuclides.

Introduction

In most nuclear countries, the disposal of longer-lived, intermediate level radioactive waste (ILW), a component of Higher Activity Waste (HAW) in the radioactive waste inventory, will be to a deep geological disposal facility (GDF). A GDF will employ a multiple engineered barrier system (EBS), intended to isolate and contain the waste for sufficient time to allow the majority of the radioactivity to decay (DEFRA *et al.*, 2008; Morris *et al.*, 2011; RWM, 2016a). Most EBS concepts include encapsulation of the wastes in cement within steel drums, which are then placed into an excavated vault. Upon re-saturation with groundwater, chemical conditioning will be achieved by a cementitious backfill of the vaults to provide a dominantly anoxic and high pH environment that enhances sorption and reduces radionuclide mobility (Holopainen, 1985; Berner, 1992; Crossland and Vines, 2001; RWM, 2015; Duro *et al.*, 2020).

In ILW, uranium (U) will typically be the dominant radionuclide by mass (RWM and NDA, 2015). Due to the long half-life of uranium (^{238}U 4.468 x10^9 y) and of its resultant decay chain elements, it is important to understand the environmental behavior of U to support implementation of a GDF. Redox cycling of U exerts a major control on its mobility. Under oxic conditions uranium, as U(VI), can form mobile carbonate complexes (Clark *et al.*, 1995); although transport is typically limited by sorption. The formation of stable U(VI) colloids at elevated pH has also been demonstrated (Bots *et al.*, 2014; Smith *et al.*, 2015). In contrast, following the onset of anoxic conditions post-closure of a GDF, sparingly soluble U(IV), often precipitated as U(IV) oxide phases, is expected to dominate (Lloyd *et al.*, 2005). In addition, the hyperalkaline conditions (pH >12.5) in a GDF can reduce the mobility of uranium by formation of uranyl silicates and uranate phases which may sorb to cementitious phases (Wellman *et al.*, 2007; Bots *et al.*, 2014), although stable U(IV) silicate colloids have also recently been reported under alkaline conditions (Neill *et al.*, 2018). A mix of both U(VI) and U(IV) species may co-exist in the EBS; an improved understanding of their different immobilization pathways is important for post-closure modelling. Both, U(IV) and U(VI), can form strong, insoluble complexes with phosphates (Rui *et al.*, 2013; Mehta *et al.*, 2015), which may be present, e.g. from the nuclear clean-up process (Thomas and Macaskie, 1996; Chambers *et al.*, 2004; RWM, 2016b) or the surrounding host rock (Porder and Ramachandran, 2013). There has been documentation of U(V) species in environmental studies, but it typically

disproportionates (Renshaw *et al.*, 2005; Vettese *et al.*, 2020). The transport behavior of uranium may be further complicated by the presence of organic ligands, such as the decontamination agents ethylenediaminetetraacetic acid (EDTA) or nitriloacetic acid (NTA) that may be disposed of with the wastes (Francis, 1998; Hummel *et al.*, 2005; Suzuki and Suko, 2006). Of particular interest, with respect to the disposal of ILW, are cellulosic items which are present at around 1% by mass of the total ILW in some wastes (IAEA, 2003; NDA and DEFRA, 2014). Under alkaline GDF conditions, cellulosic wastes are expected to undergo alkaline hydrolysis (Machell and Richards, 1957; Greenfield *et al.*, 1992; Glaus *et al.*, 1999; Knill and Kennedy, 2003), resulting in the production of a range of organic degradation products, of which isosaccharinic acid (ISA), a polyhydroxy ligand, is predicted to dominate (Whistler and BeMiller, 1958; van Loon and Glaus, 1998; Knill and Kennedy, 2003; Pavasars *et al.*, 2003; Glaus and van Loon, 2008). ISA sorbs weakly to surfaces within the cementitious wastes (Bradbury and Sarott, 1995; van Loon *et al.*, 1997) and is known to form stable complexes with radionuclides, such as uranium, which could in turn increase their mobility (Baston *et al.*, 1994; Rao *et al.*, 2004; Warwick *et al.*, 2004). ISA has the potential to be degraded, e.g. by microbial activity, and thus understanding the biogeochemical influence of microbial ISA degradation on uranium speciation, and its impact upon transport behavior under GDF conditions, is important to help develop an understanding of how waste-derived uranium could be affected by processes occurring in the GDF on the long term.

Previous biogeochemical studies have focused on the removal of $U(VI)_{(aq)}$ from solution in the absence of strong chelating agents in the context of treatment of contaminated land. These studies used electron donor additions to stimulate microbial U(VI) reduction that promoted the formation of insoluble U(IV) (Lovley *et al.*, 1991; Newsome *et al.*, 2015a). Since ISA may be a potentially significant organic substrate in ILW that could control the fate of U(VI) in and around the GDF, its role as an electron donor and carbon source stimulating microbial metabolism needs to be understood. Indeed, anaerobic microbial ISA degradation has been investigated under a range of biogeochemical conditions and pH values. Under the oxygen-depleted conditions typically expected after closure of a GDF, the oxidation of ISA can be coupled to the reduction of a range of alternative electron acceptors present in the wastes (Bassil *et al.*, 2015b; a; Kuippers *et al.*, 2015; Rout *et al.*, 2015), which may be incomplete at high pH (=10) due to diminishing energy yield when coupled to low redox potential electron acceptors, such as sulfate (Bassil *et al.*, 2015b; a; Rout *et al.*, 2015). Complete degradation was observed under a range of conditions with Fe(III) supplied as an electron acceptor, which may occur naturally in the geosphere and might also be produced *in situ* from the corrosion of steel present in ILW and engineering materials used in GDF construction (Lovley and Phillips, 1986; Konhauser, 1997; Duro *et al.*, 2014). Alternatively, some metal-

reducing bacteria directly utilize U(VI) as an electron acceptor, potentially leading to its reductive precipitation as U(IV). To date, there have been no studies examining the role of U(VI) during microbial degradation of ISA, both as a potential complexant and/or electron donor, under conditions relevant to the near and far field of a GDF.

In this study, enrichment cultures growing on ISA were used to represent potential biogeochemical conditions in the pH neutral far field environment surrounding a GDF. The focus was to investigate the fate of U(VI)$_{(aq)}$, when ISA was used as fermentation substrate, and to compare these results to data from an ISA-degrading, Fe(III)-reducing microbial enrichment. A microbial consortium that is expected to be adapted to such biogeochemical conditions, was retrieved from soil samples from an alkaline legacy lime workings site at Harpur Hill, Buxton, UK, a well characterized system and potential analogue for an evolved GDF environment (Williamson *et al.*, 2013). Uranium was removed from solution under both conditions, although the fate of the radionuclide depended on the culturing conditions. Collectively, these data highlight the potential importance of microbial processes in influencing radionuclide mobility in the far field surrounding a GDF (alongside other relevant processes).

Materials and methods

Sediments. Shallow subsurface sediment samples (approximately 20 cm depth and pH 7.5) were collected at the margins of an alkaline legacy lime workings site at Harpur Hill, Buxton, U.K., a potential analogue site representative of the alkali-disturbed zone surrounding a GDF that is known to contain ISA-degrading bacteria (Williamson *et al.*, 2013; Bassil *et al.*, 2015b; Kuippers *et al.*, 2015). The sediment was kept in the dark at 4°C until use.

Ca(ISA)$_2$ preparation. $Ca(ISA)_2$ was prepared from α-lactose monohydrate and $Ca(OH)_2$ following the protocol of Vercammen et al. (Vercammen *et al.*, 1999).

Fe(III) oxyhydroxide preparation. Fe(III) oxyhydroxide was produced according to the method of (Schwertmann and Cornell, 2000), briefly, 0.6 M $FeCl_3$ was hydrolyzed at pH 7, with six washing steps with 18Ω de-ionized water and the Fe(III) suspension was standardized using ICP analysis.

ISA-degrading, Fe(III)-reducing and fermenting enrichments. Stable enrichment cultures were obtained using a 1% (v/v) sediment inoculum and minimal medium (pH 7), approaching far field conditions of a GDF. The media contained 30 mM $NaHCO_3$, 4.7 mM NH_4Cl, 4.4 mM $NaH_2PO_4{\cdot}H_2O$, 1.3 mM KCl, and 10 mL L^{-1} of mineral and vitamin stock solutions (Lovley *et al.*, 1984). $Ca(ISA)_2$ was added as the sole added carbon source

and electron donor to a final concentration of 3.5 mM. To create an ISA-degrading and Fe(III)-reducing enrichment culture, approximately 30 mmol L^{-1} Fe(III) oxyhydroxide was added to one set of enrichment cultures, as the sole added electron acceptor, whilst a second set of ISA-fermenting enrichment cultures was grown without added Fe(III) oxyhydroxide. Microorganisms able to degrade ISA were selected via periodic sub-culturing (1% v/v inoculum) in fresh medium, typically every four weeks. Stable enrichment cultures were obtained after 12 consecutive transfers for inoculation into U(VI)-containing media.

Preparation of experimental cultures with ISA and U(VI). Enrichment cultures, approaching potential far field GDF conditions, were prepared with 30 mL anoxic medium at pH 7 containing 3.5 mM ISA. Fe(III) oxyhydroxide (30 mmoles L^{-1}) was added to the "U(VI)-ISA, Fe(III)-reducing" cultures, and these were also supplemented with 1 mM U(VI) (added as a spike of UO_2^{2+} in 0.001 M HCl) after autoclaving. A parallel set of "U(VI)-ISA fermentation" cultures without added Fe(III), and with 1 mM U(VI) as the sole electron acceptor were prepared. Finally, an inoculum (1% v/v) was added from the two stable enrichment cultures prepared with and without Fe(III), respectively, to initiate experiments. Controls were also prepared, containing the same media as above with an autoclaved (sterile) inoculum, no inoculum, or no U(VI). All serum bottles were incubated in the dark at room temperature. Periodically, samples were withdrawn and analyzed using a range of geochemical and spectroscopic techniques.

Exploring the mechanism of U(VI) reduction. Here, we explored the fate of U(VI) in Fe(III)-reducing incubations that had reached peak Fe(II) levels and were then either sterilized (autoclaved) or left microbially active, prior to the addition of 1 mM UO_2^{2+} (in 0.001 M HCl). After further incubation for 30 days, the solids were centrifuged anoxically and analyzed by U L_{III}-edge X-ray absorption spectroscopy (XAS) on beamline B18 at Diamond Light Source.

Geochemical characterization. Periodically, samples were withdrawn using anaerobic, aseptic techniques and pH, E_h, Fe(II)/Fe(III), U_{total} and U(VI) were measured before preserving the samples at -80°C for further analysis. Microbial Fe(III) reduction was measured using the ferrozine assay (Lovley and Phillips, 1987). Total uranium in solution was quantified with inductively-coupled plasma mass spectrometry (ICP-MS) and on select samples U(VI) in solution was quantified spectrophotometrically with 2-(5-bromo-2-pyridylazo)-5-diethylaminophenol at 578 nm (Johnson and Florence, 1971). ISA, organic acids, sulfate and phosphate were analyzed by ion exclusion high performance liquid ion chromatography (IE-HPLC), using a Dionex ICS5000 (SI section S1 for methodological details).

16S rRNA gene sequencing. 16S rRNA gene sequencing was performed with the Illumina MiSeq platform (Illumina, San Diego, CA, USA) using a Roche 'Fast Start High Fidelity PCR System' (Kuippers *et al.*, 2018). The raw sequencing data were deposited at the NCBI Sequence Read Archive (http://www.ncbi.nlm.nih.gov/sra/) with the accession numbers SRR7769831 – SRR7769835.

Mineralogical characterization. All preparation and analyses were performed under anaerobic conditions. Mineral phase identification was carried out using powder X-ray diffraction (XRD) crystallography on a Bruker D8 Advance using an anaerobic cell. Environmental Scanning Electron Microscopy (FEG ESEM, FEI Quanta 650) and Transmission Electron Microscopy (FEG TEM, Philips CM200) with selected area electron diffraction (SAED) were also used to characterize samples.

U(VI) speciation and coordination analysis in solids. X-ray Absorption Spectroscopy (XAS) was used to determine speciation and coordination of uranium in solids sampled at incubation end points. XAS data were collected for the L_{III}-edge and M_{IV}-edge of uranium. For studies of the U M_{IV}-edge High-Energy Resolution Fluorescence Detection X-Ray absorption near edge structure (HERFD XANES; Kvashnina *et al.*, 2013, 2014), end-point samples were centrifuged and prepared in an anaerobic holder. Spectra were collected on the ID26 beamline at the European Synchrotron Radiation Facility (ESRF) in Grenoble (Gauthier *et al.*, 1999), using a Si(111) monochromator and an X-ray emission spectrometer (Glatzel *et al.*, 2013). The U M_{IV}-edge HERFD XANES spectra were normalized according to their maxima, before analysis using Athena linear combination fitting to further quantify the likely proportion of uranyl(IV), uranyl(V) and uranyl(VI) in the samples (Ravel and Newville, 2005).

For U L_{III}-edge XAS, samples were centrifuged and diluted with cellulose to a final concentration of approximately 1% U w/w to form a pressed pellet. All samples were prepared under strictly anaerobic conditions and stored under argon atmosphere at -80 °C until analysis in a cryostat. Samples and standards (schoepite UO_3 and uraninite UO_2) were collected in fluorescence or transmission mode. Background subtraction was performed using Athena and Demeter software (Ravel and Newville, 2005). Shells and multiple scatterers (MS) were only included in the final fits, when they statistically improved the model as assessed by the F-test (Downward *et al.*, 2007).

Results and Discussion

Microbial ISA degradation has the potential to impact on the fate and speciation of uranium in the geosphere surrounding a GDF. To test this, anoxic, stable enrichment cultures were set up at pH 7 containing ISA as the sole electron donor and carbon source, and aqueous U(VI). The enrichment cultures were prepared from sediments collected at Harpur Hill, Buxton in media selective for ISA-fermenting and ISA-degrading, Fe(III)-reducing conditions with U(VI).

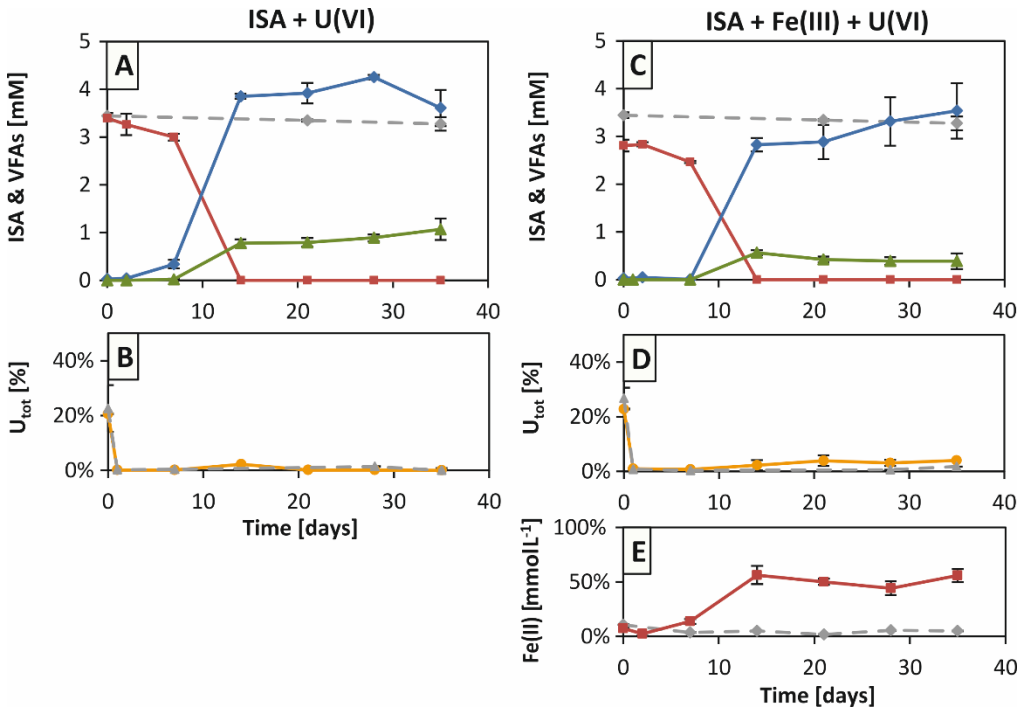

Figure 1. Solution chemistry of U(VI)-ISA fermentation (left panel) and U(VI)-Fe(III)-reducing cultures (right panel), both with 1 mM U(VI). Panel A & C: IC results for ISA (red line), acetate (blue line), butyrate (green line) and ISA in sterile control (grey dashed line); B & D: ICP MS results for total uranium in solution (yellow line) and sterile control (grey dashed line); E: Ferrozine results for Fe(II) in solution for microbially active Fe(III)-reducing culture (red line) and sterile control (grey dashed line). Note: results for $U(VI)_{(aq)}$ analyses using Bromo PADAP are presented in SI Section S1, Figure S6).

Solution chemistry. There was a lag of two days in both microbial enrichment experiments (with and without added Fe(III)) before a decrease in the ISA concentrations was observed. ISA was fully depleted by 14 days (Figure 1 A, C). In contrast, no decrease in soluble ISA concentration was observed in the heat-sterilized control incubations (Figure 1 A, C; SI Figure S1). The decrease in ISA concentration in the microbial enrichments was accompanied by a drop in redox potential to -110 mV in ISA-fermenting treatments and to -200 mV in treatments amended with Fe(III) (SI Figure S2). In the ISA-fermenting experiment, the pH remained broadly constant and in the Fe(III)-reducing experiment, modest generation of alkalinity was evident as the pH increased from 7.1 to 7.4 (SI Figure S3). No changes in E_h or pH were observed in abiotic controls (SI Figure S2 & S3). In microbially active incubations, an increase in concentrations of volatile fatty acids (VFAs; dominated by acetate

and lower concentrations of butyrate) was noted during ISA degradation (Figure 1 A, C). VFA production plateaued in both treatments at day 14, when ISA was depleted, and the amount of carbon converted to VFAs was slightly higher in the fermentation experiment at 53% ±1.5% compared to 45% ±0.5% in the Fe(III)-reducing experiment. Fe(II) ingrowth to solids (0.5 N HCl-extractable) in the Fe(III)-reducing incubations was only detected in biotic experiments. Here, Fe(II) production started after a lag phase of 7 days and continued to increase until day 14 when the concentration plateaued at approximately 56% ±3% (16 mmol L^{-1}) of the 0.5 N HCl-extractable Fe(II) fraction (Figure 1E and SI Figure S4). In addition, the total 0.5 N HCl-extractable iron fraction (Fe(II) + Fe(III)) decreased from a peak of 30 mmol L^{-1} at the start of the experiment by approximately 25% ±5% over the course of the incubation time (SI Figure S5), indicating formation of recalcitrant Fe(II)/Fe(III)-bearing solids. XRD analysis at the end of the incubation confirmed formation of siderite ($FeCO_3$) and vivianite ($(Fe_3PO_4)_2 \cdot 8H_2O$) in the incubations (SI Figure S11). Overall, ISA degradation in the Fe(III)-reducing experiment was considered to proceed via a mixed microbial community of fermenting and Fe(III)-reducing bacteria. However, the Fe(III)-reducing experiments showed a 10% decrease in the amount of carbon converted from ISA to VFAs compared to the U(VI)-ISA fermentation experiment, and following depletion of ISA the amount of VFAs decreased further, both indicators for continued oxidation of fermentation products to CO_2 coupled to Fe(III) reduction.

The concentration of total uranium (added as 1 mM U(VI)) in culture supernatants was monitored using ICP-MS (Figure 1 B, D), and spectrophotometric analysis of U(VI) was consistent with these results (SI Figure S6). At the start of incubation, U(VI) was removed rapidly from solution, before ISA degradation was detected. This rapid removal of uranium was also noted in sterile control incubations, indicating oversaturation of the system was occurring (Figure 1 B, D & SI Figure S6). XRD analysis of the uranium precipitate revealed formation of a uranyl phosphate in sterile systems (SI Figure S11), potentially due to complexation with phosphate (1 mM) from the medium (Langmuir, 1978). However, U(VI) adsorption to ferrihydrite in the Fe(III)-amended experiment could not be excluded (Waite *et al.*, 1994). When ISA levels started to decrease in the biotic experiments, a small proportion was concomitantly remobilized in both the ISA-fermenting and Fe(III)-reducing experiments; 2% and 13% U(VI), respectively. In the ISA-fermenting experiment, this U(VI) release was transient and removal was essentially complete by 35 days. By contrast, in the Fe(III)-reducing system, a small proportion (approximately 4% uranium) remained in solution throughout the remainder of the experiment. The spectrophotometric assay for U(VI) suggested the re-solubilized uranium was dominated by U(VI). Finally,

comparison of the U(VI)-amended biotic experiments with controls that did not contain uranium (SI Figure S7), showed that uranium did not impede the rates of ISA biodegradation.

***Solid phase characterization*.** Biominerals that formed were characterized using XRD, TEM and ESEM. In addition, XAS was used to define the average U(VI) oxidation state and coordination environment in key samples, including the collection of U M_{IV}-edge (SI Figure S8) and U L_{III}-edge (SI Figure S9) spectra. ICP MS data showed that in all microcosms the majority of uranium precipitated at the start of the incubation. XRD analysis on the sterile controls indicated this was potentially a uranyl phosphate phase similar to autunite (SI Figure S10 and S11).

ISA-fermenting experiment with U(VI)

In the ISA-fermenting enrichment culture, brief remobilization of approximately 2% of uranium between day 7 and 21 was observed, with complete removal of uranium from solution by the end of the incubation period. Using XRD, the precipitate was identified as a uranyl phosphate (either K- or Na-autunite), a similar structure to the precipitate in the sterile controls (SI Figure S11). Further characterization by ESEM showed well-defined spherules with an average size of 800 nm ±14 nm that appeared to consist of smaller plates (SI Figure S13A). TEM images confirmed a typical autunite-like morphology (Gudavalli *et al.*, 2013), and revealed individual plates ranging in size from 15 to 40 nm that aggregated into spherules (Figure 2A). EDS analysis of the corresponding TEM images identified O, P, U and trace Na (Figure 2B), consistent with metanatroautunite. U M_{IV}-edge spectroscopy confirmed U(VI) was dominant (SI Figure S8), with linear combination fitting (LCF) of the U M_{IV}-edge HERFD XANES showing approximately 98% U(VI) in the solid phase by the end of the incubation period (SI Figure S10; Table S1). EXAFS analyses were informed by the relevant U(VI)-phosphate literature (Locock and Burns, 2003) and the best fit contained 2 axial O backscatterers at 1.78 Å, 4 equatorial O backscatterers at 2.43 Å, and 3 P backscatterers at 3.62 Å (Table 1). This model suggests a U(VI) uranyl species coordinated by 3 phosphate ions around the equatorial plane, consistent with the autunite-like U(VI)-phosphate identified from XRD analysis (Singh *et al.*, 2012; Mehta *et al.*, 2016).

Interestingly, although uranium was not reduced in the U(VI)-ISA fermentation experiment, TEM EDS analysis showed significant accumulation of U- and P-containing precipitates on the cells (SI Figure S14). These uranium precipitates could have complexed with ligands in the microbial cell surface, such as carboxyl, amine, hydroxyl, phosphate and sulfhydryl groups (Beveridge and Murray, 1980; Lloyd and Macaskie, 2000). Thus,

uranium in the U(VI)-ISA fermentation experiment was primarily mineralized as an U(VI)-phosphate mineral which seemed partially associated with the microbial cell surface.

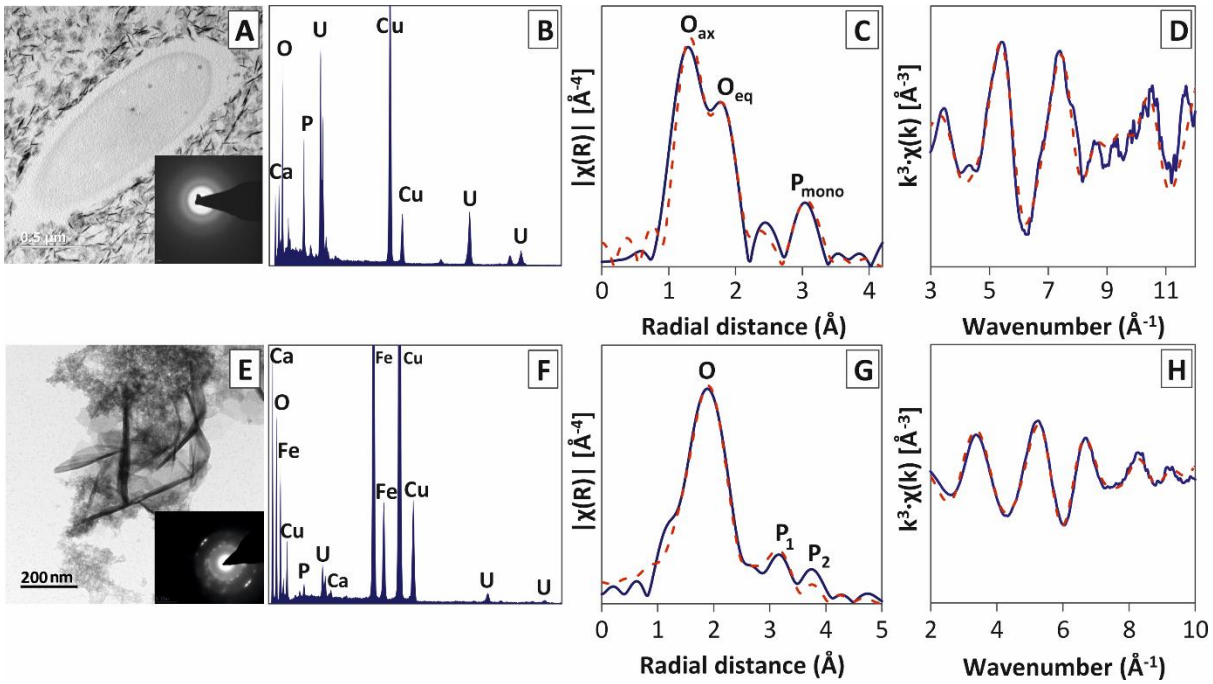

Figure 2. Mineralogical analysis of ISA-fermenting U(VI) experiment (A-D) and ISA degradation, Fe(III)-reducing U(VI) experiment (E-H) both with 1 mM U(VI). In detail: A) & E) TEM images with SAED; B) & F) corresponding EDS of TEM images; C) & G) non-phase shift corrected U L_{III}-edge EXAFS data and D) & H) corresponding k^3 weighted Fourier transform of EXAFS data. EXAFS data are represented by blue lines and corresponding fits by red dotted lines.

Sample	Scattering path	Coordination number	Atomic distance (Å)	Debye-Waller factor σ^2 (Å^2)	R-factor	ΔE_0
U(VI)-ISA fermentation						
	O_{ax}	2	1.76(1)	0.002(1)	0.0018	2.0(21)
	O_{eq}	4.5	2.26(1)	0.004(1)		
	$P_{monodentate}$	3	3.62(3)	0.005(3)		
	$O_{ax\text{-}rattle}$	2	3.52(1)	0.008(1)		
	$O_{ax\text{-}non\text{-}forward}$	2	3.52(1)	0.004(1)		
	$O_{ax\text{-}forward}$	2	3.52(1)	0.004(1)		
U(VI)-ISA + Fe(III)						
	O_{eq}	3	2.27(2)	0.006(3)	0.0013	5.2(14)
	O_{eq}	5	2.43(2)	0.005(2)		
	$P_{bidentante}$	1.2	3.14(2)	0.005(2)		
	$P_{monodentante}$	1.8	3.71(3)	0.005(2)*		

Table 1. EXAFS fit parameters for U(VI)-ISA degradation experiments with Fe(III) and without Fe(III) added both with 1 mM U(VI). ΔE_0 is energy shift from calculated Fermi level in eV. The amplitude factor ($S0^2$) was fixed as 1.0 for the U(VI)-ISA + Fe(III) sample and 0.9 for the U(VI)-ISA fermentation sample. Indices are: $_{ax}$ for axial atoms and $_{eq}$ for equatorial atoms. * indicates linked to parameter above.

U(VI)-Fe(III)-reducing, ISA biodegradation experiment

At the start of the Fe(III)-reducing experiment, uranium was precipitated as a uranyl phosphate, similar to the ISA-fermenting experiment. After the incubation period, no crystalline uranium phase was detected by XRD in

the microbially active incubations, whereas in the sterile, Fe(III)-reducing control a uranyl precipitate was identified (SI Figure S11). Instead, in the biotic experiment, siderite ($FeCO_3$) and vivianite ($(Fe_3PO_4)_2 \cdot 8H_2O$) had formed. U M_{IV}-edge HERFD XANES data for the experiment end point confirmed the uranium was present predominantly as U(IV) (LCF showed 97% U(IV); SI Figure S10; SI Table S1). In ESEM (SI Figure S13B) and TEM images (Figure 2E; SI Figure S15) these U(IV) particles appeared as thin sheets agglomerated into clusters with a clearly different morphology to the end point uranium precipitate in the ISA fermentation experiment. Corresponding EDS analysis from several different areas of these clusters showed O, Fe, P, U and Ca (Figure 2F).

Again, EXAFS fitting for the sample was informed by relevant published literature and a good fit was achieved with a split shell of three equatorial O backscatterers at 2.29 Å, five equatorial O backscatterers at 2.42 Å, and two P backscatterer shells containing 1.2 atoms at 3.01 Å and 1.8 atoms at 3.75 Å (Figure 2G, H; Table 1). This model is consistent with a range of previously described U(IV)-phosphate structures, including a nanocrystalline ningyoite-like structure (Dusausoy *et al.*, 1996; Newsome *et al.*, 2015a) and phosphate coordinated monomeric U(IV) (Boyanov *et al.*, 2011; Bargar *et al.*, 2013; Alessi *et al.*, 2014). Due to similar bond distances and coordination numbers, delineating between these phases to identify the exact U(IV)-phosphate phase is not possible using solely EXAFS and so from hereon, the U(IV)-phosphate phase present in this study will be referred to as 'ningyoite-like'. In a sterile control prepared alongside with Fe(III) and U(VI), U(VI) reduction was absent, indicating U(VI) reduction to be a microbially-mediated process in the U(VI)-Fe(III)-reducing experiment. This is in contrast to the biotic U(VI)-ISA fermentation experiment, where U(VI) reduction was circumvented. Microbially-mediated mechanisms for U(VI) reduction include direct enzymatic reduction where U(VI) serves as an alternative electron acceptor (Lovley *et al.*, 1991; Gorby and Lovley, 1992; Fredrickson *et al.*, 2000), or indirectly microbially-mediated reduction of an electron acceptor, such as via reduction of Fe(III), which generates reducing capacity via Fe(II) for abiotic U(VI) reduction (Jeon *et al.*, 2005; O'Loughlin *et al.*, 2010; Veeramani *et al.*, 2011). To further explore the mechanism of reduction, an additional set of Fe(III)-reducing microcosms was set up and U(VI) was added to these microcosms after Fe(III) reduction was complete. One set of these controls was autoclaved before U(VI) was added to study abiotic U(VI) reduction mediated by biogenic Fe(II), whilst U(VI) was added to the other control in a microbially active state. After incubation for a month, U L_{III}-edge XANES indicated that U(VI) was reduced to U(IV) only with a viable microbial inoculum (SI Figure S12), suggesting that direct microbial processes catalyzed U(VI) reduction in the presence of Fe(II)-bearing mineral phases.

Microbial community analysis. 16S rRNA gene profiles were obtained by Illumina sequencing for all treatments at the end of incubation (Figure 3), to identify the microorganisms that may have been involved in controlling the biogeochemical fate of uranium. Sequence analyses of the original, pH 7.5 soil samples, retrieved from the potential analogue site, Harpur Hill, indicated a complex background microbial community dominated by sequences most closely affiliated with the classes Betaproteobacteria (22.3% of total sequence abundance) and Bacteroidia (16.6% of total sequence abundance; Figure 3). Alpha-rarefaction curves showed a significant decrease in species diversity after enrichment from over 1,000 observed operational taxonomic units (OTUs) in the original sediments, to approximately 135 OTUs in the ISA-fermenting experiment and 150 OTUs in the Fe(III)-reducing experiment (SI Figure S16). At the end of the experiments, both treatments were dominated by a class most closely affiliated with members of Clostridia (over 40% of total sequences), but close examination of the 16S rRNA gene sequences revealed a marked difference between the treatments at the family level.

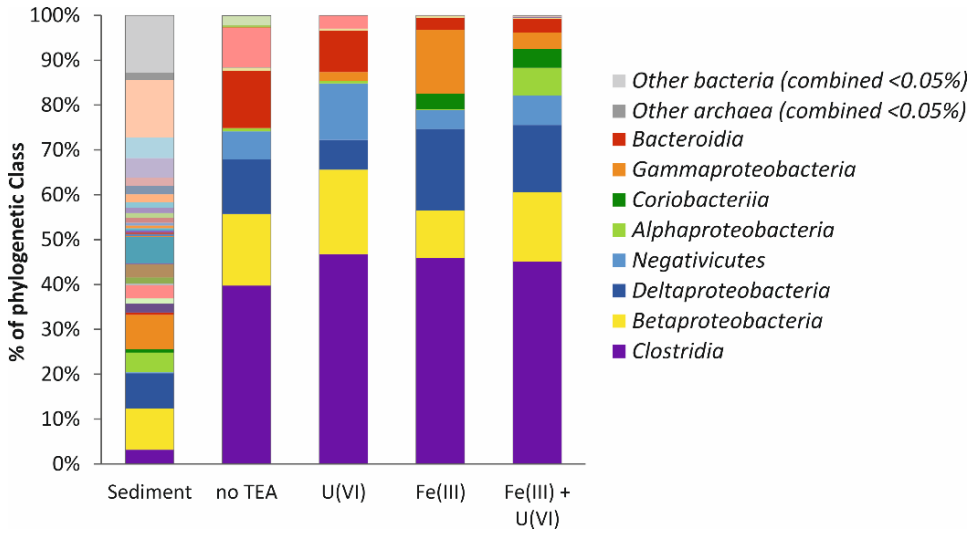

Figure 3. Microbial community fingerprinting showing the most important phylogenetic classes within sediments before incubation, alongside bioreduced ISA-fermenting and ISA, Fe(III)-reducing cultures with and without added U(VI) after 14 days of incubation performed by using 16S rRNA gene sequencing.

Focusing on the ISA-fermenting enrichment with U(VI), this experiment was characterized, in addition to the strong enrichment of Clostridia (46.8% of genes detected), by a high relative abundance of sequences associated with members from the class Betaproteobacteria (18.7% of genes detected) and an enrichment of sequences affiliated with the class Negativicutes (of 12.8% of genes detected). The Negativicutes were comprised of sequences from the family *Veillonellaceae* (98% match). Another significant class comprised the Bacteroidia (12.5% of genes detected), of which most sequences were associated with a member from the *vadinBC27*

319 *wastewater sludge group* (approximately 73% of this class) from the family *Rikenellaceae*. The microbial
320 profile of the ISA-fermenting culture without added U(VI) comprised the same classes and species.

321 By contrast, in the U(VI)-amended Fe(III)-reducing enrichment, the second most abundant class (after the
322 Clostridia) comprised of members belonging to the Deltaproteobacteria (14.7% of total sequence abundance).
323 Two families were enriched within this class, with the majority related to the Fe(III)-reducing family
324 *Geobacteraceae* (11.8% of total sequence abundance, 97% match) and a smaller proportion related to species
325 from the sulfate-reducing (and Fe(III)-reducing) *Desulfovibrionaceae* (3% of total sequence abundance, 98%
326 match). *Geobacter* sp. are dissimilatory metal-reducing bacteria that can couple oxidation of organic carbon to
327 the reduction of a wide range of terminal electron acceptors, including Fe(III) and U(VI) (Lovley *et al.*, 1991).
328 These species were not enriched in the -ISA-fermenting cultures which were established without an alternative
329 electron acceptor. As discussed, the controls prepared to study the mechanism of U(VI) reduction indicated that
330 enzymatic U(VI) reduction occurred in these microcosms, and indeed several potential candidates, known to be
331 capable of enzymatic U(VI) reduction, were enriched, comprising *Geobacter* spp. (Lovley *et al.*, 1993; Vali *et*
332 *al.*, 2004; Shelobolina *et al.*, 2008), *Clostridia* spp. (Francis *et al.*, 1994; Boonchayaanant *et al.*, 2009) and
333 members of the family *Veillonellaceae* from the Negativicutes (Woolfolk and Whiteley, 1962; Gihring *et al.*,
334 2011). However, *Clostridia* spp. and *Veillonellaceae* spp. do not appear to be associated with the reduction of
335 U(VI), as these species were also strongly enriched in the U(V)-ISA-fermenting experiment, where U(VI)
336 reduction was absent. This implies species affiliated with *Geobacteraceae* potentially played an important role
337 in the reduction of U(VI) to U(IV) in these systems.

338 Overall, anaerobic microbial enrichment cultures fueled by ISA degradation, were able to couple the oxidation
339 of ISA or its degradation products to the reduction of U(VI)-phosphate, when enriched on Fe(III) as an electron
340 acceptor, whilst no U(VI) reduction was observed in the cultures incubated under ISA-fermenting conditions
341 alone. In addition, 16S rRNA gene profiling identified *Geobacter* species as potential candidates involved in
342 enzymatic U(VI) reduction, alongside other metal-reducing bacteria including species from the
343 *Desulfovibrionaceae* and *Veillonellaceae*. These findings shed light on how the subsurface microbial
344 community in and around a GDF may adapt to changing geochemical environments, and highlight the
345 availability of terminal electron acceptors as a controlling factor in these systems. The microbial community
346 structure in turn can have a profound impact on the oxidation state of uranium (and potentially other
347 radionuclides) and therefore the speciation of end-member precipitates. Although early work on microbial
348 U(VI) reduction noted uraninite (UO_2) as the dominant end point mineral, U(IV)-phosphates have also been

observed more recently as the products of microbial U(VI) reduction, especially in the presence of aqueous phosphate (Bernier-Latmani *et al.*, 2010; Lee *et al.*, 2010; Newsome *et al.*, 2015a) or after reduction of a U(VI) phosphate mineral phase (Khijniak *et al.*, 2005; Rui *et al.*, 2013). Although the autunite-like mineral that was precipitated under ISA-fermenting conditions is a stable end product and a sink for U(VI) that can persist over geological timescales (Langmuir, 1978; Sato *et al.*, 1997; Jerden and Sinha, 2003), the ningyoite-like precipitate from U(VI)-Fe(III)-reducing conditions is considered more recalcitrant towards oxidation and thus remobilization (Finch and Murakami, 1999; Jerden and Sinha, 2003; Pinto *et al.*, 2012; Newsome *et al.*, 2015b; a). Additional reducing capacity, associated with the Fe(II)-bearing minerals vivianite and siderite, was also identified, and both minerals have been shown to mediate the reduction of priority radionuclides, e.g. Tc(VII) and Np(V), and leading to their reductive immobilization (Lloyd *et al.*, 2000; Law *et al.*, 2010; McBeth *et al.*, 2011; Thorpe *et al.*, 2014).

Our work suggests that ningyoite is an ideal end member of U(VI) bioreduction associated with anoxic environments in radioactive waste disposal, and that biogeochemical factors (e.g. bioavailable Fe(III) and phosphate concentrations) can promote its formation within a 'bio-barrier', enhancing the strength-in-depth approach afforded by the multiple barriers of the EBS and geosphere.

Acknowledgements

This work was supported by Radioactive Waste Management Limited (RWM). The authors would like to thank NERC for additional funding under the OPTIUM consortium (NE/R011230/1). JRL also acknowledges the financial support of the Royal Society and the EU MIND programme under "Euratom2014–2015" and the call "NFRP-06-2014: Supporting the implementation of the first of-a-kind geological repositories". We thank both Diamond Light Source (SP12767, SP13599) and European Synchrotron Radiation Facility (EV/192) for beamtime and EnvRadNet for travel and subsistence to ESRF. We would like to thank Dr Z Azlam of the University of Leeds LENNF facilities for TEM support. Further thank goes to Paul Lythgoe, Alastair Bewsher and John Waters for analytical support and Kurt Smith for assistance with data analysis.

Competing financial interests

The authors declare no competing financial interest.

Author contributions

GK – primary investigator, preparation and monitoring of experiments, data acquisition, analysis and interpretation, manuscript drafting; LT, PB, KM, KK and – support with XANES & EXAFS data collection,

analysis and interpretation; CB – sample analysis for microbial ecology (sequencing); KM, LT – manuscript review; JRL Planning experiments with GK, data interpretation, review and editing of manuscript.

Associated Content

Supporting Information

Methodological details, pH and E_h data, Fe(II) + Fe(III) data, XRD data, additional TEM figures, α-rarefaction curves, additional XANES and EXAFS fitting results and parameters used for fitting.

References

Alessi, D.S., Lezama-Pacheco, J.S., Stubbs, J.E., Janousch, M., Bargar, J.R., Persson, P. and Bernier-Latmani, R. (2014) The product of microbial uranium reduction includes multiple species with U(IV)–phosphate coordination. *Geochimica et Cosmochimica Acta*, **131**, 115–127. Pergamon.

Bargar, J.R., Williams, K.H., Campbell, K.M., Long, P.E., Stubbs, J.E., Suvorova, E.I., Lezama-Pacheco, J.S., Alessi, D.S., Stylo, M., Webb, S.M., Davis, J.A., Giammar, D.E., Blue, L.Y. and Bernier-Latmani, R. (2013) Uranium redox transition pathways in acetate-amended sediments. *Proceedings of the National Academy of Sciences*, **110**, 4506–4511. National Academy of Sciences.

Bassil, N.M., Bewsher, A.D., Thompson, O.R. and Lloyd, J.R. (2015a) Microbial degradation of cellulosic material under intermediate-level waste simulated conditions. *Mineralogical Magazine*, **79**.

Bassil, N.M., Bryan, N. and Lloyd, J.R. (2015b) Microbial degradation of isosaccharinic acid at high pH. *The ISME Journal*, **9**, 310–320. Nature Publishing Group.

Baston, G.M.N., Berry, J.A., Bond, K.A., Boult, K.A., Brownsword, M. and Linklater, C.M. (1994) Effects of cellulosic degradation products on uranium sorption in the geosphere. *Journal of Alloys and Compounds*, **213**–**214**, 475–480.

Berner, U.R. (1992) Evolution of pore water chemistry during degradation of cement in a radioactive waste repository environment. *Waste Management*, **12**, 201–219. Pergamon.

Bernier-Latmani, R., Veeramani, H., Vecchia, E.D., Junier, P., Lezama-Pacheco, J.S., Suvorova, E.I., Sharp, J.O., Wigginton, N.S. and Bargar, J.R. (2010) Non-uraninite products of microbial U(VI) reduction. *Environmental Science & Technology*, **44**, 9456–9462. American Chemical Society.

Beveridge, T.J. and Murray, R.G.E. (1980) Sites of metal deposition in the cell wall of *Bacillus subtilis*. *Journal of Bacteriology*, **141**, 876–887.

Boonchayaanant, B., Nayak, D., Du, X. and Criddle, C.S. (2009) Uranium reduction and resistance to reoxidation under iron-reducing and sulfate-reducing conditions. *Water Research*, **43**, 4652–4664.

Bots, P., Morris, K., Hibberd, R., Law, G.T.W., Mosselmans, J.F.W., Brown, A.P., Doutch, J., Smith, A.J. and Shaw, S. (2014) Formation of stable uranium(VI) colloidal nanoparticles in conditions relevant to radioactive waste disposal. *Langmuir*, **30**, 14396–14405. American Chemical Society.

Boyanov, M.I., Fletcher, K.E., Kwon, M.J., Rui, X., O'Loughlin, E.J., Löffler, F.E. and Kemner, K.M. (2011) Solution and Microbial Controls on the Formation of Reduced U(IV) Species. *Environmental Science & Technology*, **45**, 8336–8344. American Chemical Society.

Bradbury, M.H. and Sarott, F.-A. (1995) *Sorption Databases for the Cementitious Near-Field of a L/ILW Repository for Performance Assessment*. Würenlingen & Villigen, 95-6 pp.

Chambers, A.V., Heath, T.G. and Hunter, F.M.I. (2004) *A review of the effect of the tetraphenyl-phosphonium*

ion and its degradation products on radioelement solubility under near-field conditions. Didcot, 42 pp.

Clark, D.L., Hobart, D.E. and Neu, M.P. (1995) Actinide carbonte complexes and their importance in actinide environmental chemistry. *Chemical Reviews*, **95**, 25–48. American Chemical Society.

Crossland, I.G. and Vines, S.P. (2001) *Why a cementitious repository?* 1–18 pp.

DEFRA, BERR and The devolved administrations for Wales and Northern Ireland. (2008) Managing radioactive waste safely: A framework for implementing geological disposal. 1–100.

Downward, L., Booth, C.H., Lukens, W.W. and Bridges, F. (2007) A variation of the F-test for determining statistical relevance of particular parameters in EXAFS fits. Pp. 129–131 in: *AIP Conference Proceedings*. AIP.

Duro, L., Domènech, C., Grivé, M., Roman-Ross, G., Bruno, J. and Källström, K. (2014) Assessment of the evolution of the redox conditions in a low and intermediate level nuclear waste repository (SFR1, Sweden). *Applied Geochemistry*, **49**, 192–205. Elsevier Ltd.

Duro, L., Altmaier, M., Holt, E., Mäder, U., Claret, F., Grambow, B., Idiart, A., Valls, A. and Montoya, V. (2020) Contribution of the results of the CEBAMA project to decrease uncertainties in the Safety Case and Performance Assessment of radioactive waste repositories. *Applied Geochemistry*, **112**, 13. Elsevier Ltd.

Dusausoy, Y., Ghermani, N.-E., Podor, R. and Cuney, M. (1996) Low-temperature ordered phase of CaU(PO4); synthesis and crystal structure. *European Journal of Mineralogy*, **8**, 667–674.

Finch, R. and Murakami, T. (1999) Systematics and paragenesis of uranium minerals. *Reviews in Mineralogy and Geochemistry*, **38**, 91–179.

Francis, A.J. (1998) Biotransformation of uranium and other actinides in radioactive wastes. *Journal of Alloys and Compounds*, **271**–**273**, 78–84.

Francis, A.J., Dodge, C.J., Lu, F., Halada, G.P. and Clayton, C.R. (1994) XPS and XANES studies of uranium reduction by *Clostridium* sp. *Environmental Science & Technology*, **28**, 636–639.

Fredrickson, J.K., Zachara, J.M., Kennedy, D.W., Duff, M.C., Gorby, Y.A., Li, S.M.W. and Krupka, K.M. (2000) Reduction of U(VI) in goethite (α-FeOOH) suspensions by a dissimilatory metal-reducing bacterium. *Geochimica et Cosmochimica Acta*, **64**, 3085–3098.

Gauthier, C., Solé, V.A., Signorato, R., Goulon, J. and Moguiline, E. (1999) The ESRF beamline ID26: X-ray absorption on ultra dilute sample. *Journal of Synchrotron Radiation*, **6**, 164–166. International Union of Crystallography.

Gihring, T.M., Zhang, G., Brandt, C.C., Brooks, S.C., Campbell, J.H., Carroll, S., Criddle, C.S., Green, S.J., Jardine, P., Kostka, J.E., Lowe, K., Mehlhorn, T.L., Overholt, W., Watson, D.B., Yang, Z., Wu, W.-M. and Schadt, C.W. (2011) A limited microbial consortium is responsible for extended bioreduction of uranium in a contaminated aquifer. *Applied and Environmental Microbiology*, **77**, 5955–5965. American Society for Microbiology.

Glatzel, P., Weng, T.-C., Kvashnina, K., Swarbrick, J., Sikora, M., Gallo, E., Smolentsev, N. and Mori, R.A. (2013) Reflections on hard X-ray photon-in/photon-out spectroscopy for electronic structure studies. *Journal of Electron Spectroscopy and Related Phenomena*, **188**, 17–25.

Glaus, M.A. and van Loon, L.R. (2008) Degradation of Cellulose under Alkaline Conditions: New Insights from a 12 Years Degradation Study. *Environmental Science & Technology*, **42**, 2906–2911. American Chemical Society.

Glaus, M.A., van Loon, L.R., Achatz, S., Chodura, A., Fischer, K., Loon, L.R. Van, Achatz, S., Chodura, A. and Fischer, K. (1999) Degradation of cellulosic materials under the alkaline conditions of a cementitious

repository for low and intermediate level radioactive waste Part I: Identification of degradation products. *Analytica Chimica Acta*, **398**, 111–122.

Gorby, Y.A. and Lovley, D.R. (1992) Enzymatic uranium precipitation. *Environmental Science & Technology*, **26**, 205–207.

Greenfield, B.F., Moreton, A.D., Spindler, M.W., J, W.S. and Woodwark, D.R. (1992) The effects of the degradation of organic materials in the near field of a radioactive waste repository. *Materials Research Society Symposium Proceedings*, **257**.

Gudavalli, R.K.P., Katsenovich, Y.P., Wellman, D.M., Idarraga, M., Lagos, L.E. and Tansel, B. (2013) Comparison of the kinetic rate law parameters for the dissolution of natural and synthetic autunite in the presence of aqueous bicarbonate ions. *Chemical Geology*, **351**, 299–309. Elsevier.

Holopainen, P. (1985) Crushed aggregate-bentonite mixtures as backfill material for repositories of low- and intermediate level radioactive wastes. *Engineering Geology*, **21**, 239–245. Elsevier.

Hummel, W., Mompean, F.J., Illemassène, M. and Perrone, J. (2005) *Chemical thermodynamics of compounds and complexes of U, Np, Pu, Am, Tc, Se, Ni, and Zr, with selected organic ligands*. P. in.: 1st edition. Elsevier, 1088 pp.

IAEA. (2003) *Scientific and technical basis for the geological disposal of radioactive wastes.* International Atomic Energy Agency, Vienna, 80 pp.

Jeon, B.-H., Dempsey, B.A., Burgos, W.D., Barnett, M.O. and Roden, E.E. (2005) Chemical Reduction of U(VI) by Fe(II) at the Solid−Water Interface Using Natural and Synthetic Fe(III) Oxides. *Environmental Science & Technology*, **39**, 5642–5649. American Chemical Society.

Jerden, J.L. and Sinha, A.. K. (2003) Phosphate based immobilization of uranium in an oxidizing bedrock aquifer. *Applied Geochemistry*, **18**, 823–843.

Johnson, D.A. and Florence, T.M. (1971) Spectrophotometric determination of uranium(VI) with 2-(5-bromo-2-pyridylazo)-5-diethylaminophenol. *Analytica Chimica Acta*, **53**, 73–79.

Khijniak, T. V, Slobodkin, A.I., Coker, V., Renshaw, J.C., Livens, F.R., Bonch-Osmolovskaya, E.A., Birkeland, N.-K., Medvedeva-Lyalikova, N.N. and Lloyd, J.R. (2005) Reduction of uranium(VI) phosphate during growth of the thermophilic bacterium *Thermoterrabacterium ferrireducens*. *Applied and Environmental Microbiology*, **71**, 6423–6426. American Society for Microbiology.

Knill, C.J. and Kennedy, J.F. (2003) Degradation of cellulose under alkaline conditions. *Carbohydrate Polymers*, **51**, 281–300.

Konhauser, K.O. (1997) Bacterial iron biomineralisation in nature. *FEMS Microbiology Reviews*, **20**, 315–326. Elsevier.

Kuippers, G., Bassil, N.M., Boothman, C., Bryan, N. and Lloyd, J.R. (2015) Microbial degradation of isosaccharinic acid under conditions representative for the far field of radioactive waste disposal facilities. *Mineralogical Magazine*, **79**, 1443–1454.

Kuippers, G., Boothman, C., Bagshaw, H., Ward, M., Beard, R., Bryan, N. and Lloyd, J.R. (2018) The biogeochemical fate of nickel during microbial ISA degradation; implications for nuclear waste disposal. *Scientific Reports*, **8**, 1–11.

Kvashnina, K.O., Butorin, S.M., Martin, P. and Glatzel, P. (2013) The chemical state of complex uranium oxides. *Physical Review Letters*, **111**, 1–5.

Kvashnina, K.O., Kvashnin, Y.O. and Butorin, S.M. (2014) Role of resonant inelastic X-ray scattering in high-resolution core-level spectroscopy of actinide materials. *Journal of Electron Spectroscopy and Related Phenomena*, **194**, 27–36. Elsevier B.V.

503 Langmuir, D. (1978) Uranium solution-mineral equilibria at low temperatures with applications to sedimentary
504 ore deposits. *Geochimica et Cosmochimica Acta*, **42**, 547–569.

505 Law, G.T.W., Geissler, A., Boothman, C., Burke, I.T., Livens, F.R., Lloyd, J.R. and Morris, K. (2010) Role of
506 Nitrate in Conditioning Aquifer Sediments for Technetium Bioreduction. *Environmental Science &*
507 *Technology*, **44**, 150–155. American Chemical Society.

508 Lee, S.Y., Baik, M.H. and Choi, J.W. (2010) Biogenic Formation and Growth of Uraninite (UO2).
509 *Environmental Science & Technology*, **44**, 8409–8414. American Chemical Society.

510 Lloyd, J.R. and Macaskie, L.E. (2000) Bioremediation of radionuclide-containing wastewaters. Pp. 277–327 in:
511 *Environmental Microbe-Metal Interactions* (D. Lovley, editor). American Society of Microbiology.

512 Lloyd, J.R., Yong, P. and Macaskie, L.E. (2000) Biological reduction and removal of Np(V) by two
513 microorganisms. *Environmental Science & Technology*, **34**, 1297–1301. American Chemical Society.

514 Lloyd, J.R., Renshaw, J.C., Zylstra, G.J. and Kukor, J.J. (2005) Bioremediation of radioactive waste:
515 radionuclide–microbe interactions in laboratory and field-scale studies. *Current Opinion in Biotechnology*,
516 **16**, 254–260.

517 Locock, A.J. and Burns, P.C. (2003) The crystal structure of synthetic autunite, $Ca[(UO_2)(PO_4)]2\cdot(H_2O)_{11}$.
518 *American Mineralogist*, **88**, 240–244.

519 van Loon, L.R. and Glaus, M.A. (1998) *Experimental and Theoretical Studies on Alkaline Degradation of*
520 *Cellulose and its Impact on the Sorption of Radionuclides*. Würenlingen & Villigen, 1–155 pp.

521 van Loon, L.R., Glaus, M.A., Stallone, S. and Laube, A. (1997) Sorption of isosaccharinic acid, a cellulose
522 degradation product, on cement. *Research Communications*, **31**, 1243–1245.

523 Lovley, D.R. and Phillips, E.J.P. (1986) Availability of ferric iron for microbial reduction in bottom sediments
524 of the freshwater tidal potomac river. *Applied and Environmental Microbiology*, **52**, 751–757. American
525 Society for Microbiology.

526 Lovley, D.R. and Phillips, E.J.P. (1987) Rapid assay for microbially reducible ferric iron in aquatic sediments.
527 *Applied and Environmental Microbiology*, **53**, 1536–1540.

528 Lovley, D.R., Greening, R.C. and Ferry, J.G. (1984) Rapidly growing rumen methanogenic organism that
529 synthesizes coenzyme M and has a high affinity for formate. *Applied and Environmental Microbiology*,
530 **48**, 81–87.

531 Lovley, D.R., Phillips, E.J.P., Gorby, Y.A. and Landa, E.R. (1991) Microbial reduction of uranium. *Letters to*
532 *Nature*, **350**, 413–416.

533 Lovley, D.R., Giovannoni, S.J., White, D.C., Champine, J.E., Phillips, E.J.P., Gorby, Y.A. and Goodwin, S.
534 (1993) *Geobacter metallireducens* gen. nov. sp. nov., a microorganism capable of coupling the complete
535 oxidation of organic compounds to the reduction of iron and other metals. *Archives of Microbiology*, **159**,
536 336–344. Springer-Verlag.

537 Machell, B.G. and Richards, G.N. (1957) The alkaline degradation of polysaccharides. part II. The alkali-stable
538 residue from the action of sodium hydroxide on cellulose. *Journal of the Chemical Society*, 4500–4506.

539 McBeth, J.M., Lloyd, J.R., Law, G.T.W., Livens, F.R., Burke, I.T. and Morris, K. (2011) Redox interactions of
540 technetium with iron-bearing minerals. *Mineralogical Magazine*, **75**.

541 Mehta, V.S., Maillot, F., Wang, Z., Catalano, J.G. and Giammar, D.E. (2015) Transport of U(VI) through
542 sediments amended with phosphate to induce in situ uranium immobilization. *Water Research*, **69**, 307–
543 317. Elsevier Ltd.

544 Mehta, V.S., Maillot, F., Wang, Z., Catalano, J.G. and Giammar, D.E. (2016) Effect of reaction pathway on the

545 extent and mechanism of uranium(VI) immobilization with calcium and phosphate. *Environmental*
546 *Science & Technology*, **50**, 3128–3136.

547 Morris, K., Law, G.T.W. and Bryan, N.D. (2011) Chapter 6. Geodisposal of Higher Activity Wastes. Pp. 129–
548 151 in: *Nuclear Power and the Environment* (R.M. Harrison and R.E. Hester, editors). Royal Society of
549 Chemistry.

550 NDA and DEFRA. (2014) *The 2013 UK Radioactive waste inventory: Radioactive waste composition*. Nuclear
551 Decommissioning Authority 2014, Moor Row, 14 pp.

552 Neill, T.S., Morris, K., Pearce, C.I., Sherriff, N.K., Burke, ⊥ M Grace, Chater, P.A., Janssen, A., Natrajan, L.
553 and Shaw, S. (2018) Stability, composition, and core−shell particle structure of uranium(IV)-silicate
554 colloids. *Environmental Science & Technology*, **52**, 9118–9127.

555 Newsome, L., Morris, K., Trivedi, D., Bewsher, A. and Lloyd, J.R. (2015a) Biostimulation by glycerol
556 phosphate to precipitate recalcitrant uranium(IV) phosphate. *Environmental Science & Technology*, **49**,
557 11070–11078. American Chemical Society.

558 Newsome, L., Morris, K., Shaw, S., Trivedi, D. and Lloyd, J.R. (2015b) The stability of microbially reduced
559 U(IV); impact of residual electron donor and sediment ageing. *Chemical Geology*, **409**.

560 O'Loughlin, E.J., Kelly, S.D. and Kemner, K.M. (2010) XAFS Investigation of the Interactions of U^{VI} with
561 Secondary Mineralization Products from the Bioreduction of Fe^{III} Oxides. *Environmental Science &*
562 *Technology*, **44**, 1656–1661. American Chemical Society.

563 Pavasars, I., Hagberg, J., Borén, H. and Allard, B. (2003) Alkaline degradation of cellulose: Mechanisms and
564 kinetics. *Journal of Polymers and the Environment*, **11**, 39–47.

565 Pinto, A.J., Gonçalves, M.A., Prazeres, C., Astilleros, J.M. and Batista, M.J. (2012) Mineral replacement
566 reactions in naturally occurring hydrated uranyl phosphates from the Tarabau deposit: Examples in the
567 Cu–Ba uranyl phosphate system. *Chemical Geology*, **312**–**313**, 18–26.

568 Porder, S. and Ramachandran, S. (2013) The phosphorus concentration of common rocks-a potential driver of
569 ecosystem P status. *Plant and Soil*, **367**, 41–55. Springer.

570 Rao, L., Garnov, A.Y., Rai, D., Xia, Y. and Moore, R.C. (2004) Protonation and complexation of isosaccharinic
571 acid with U(VI) and Fe(III) in acidic solutions: potentiometric and calorimetric studies. *Radiochimica*
572 *Acta*, **92**, 575–581.

573 Ravel, B. and Newville, M. (2005) ATHENA, ARTEMIS, HEPHAESTUS: data analysis for X-ray absorption
574 spectroscopy using IFEFFIT. *Journal of Synchrotron Radiation*, **12**, 537–541.

575 Renshaw, J.C., Butchins, L.J.C., Livens, F.R., May, I., Charnock, J.M. and Lloyd, J.R. (2005) Bioreduction of
576 uranium: Environmental implications of a pentavalent intermediate. *Environmental Science &*
577 *Technology*, **39**, 5657–5660.

578 Rout, S.P., Charles, C.J., Doulgeris, C., McCarthy, A.J., Rooks, D.J., Loughnane, J.P., Laws, A.P. and
579 Humphreys, P.N. (2015) Anoxic biodegradation of isosaccharinic acids at alkaline pH by natural
580 microbial communities. *PLoS ONE*, **10**, 1–17. Public Library of Science.

581 Rui, X., Kwon, M.J., O'Loughlin, E.J., Dunham-Cheatham, S., Fein, J.B., Bunker, B., Kemner, K.M. and
582 Boyanov, M.I. (2013) Bioreduction of Hydrogen Uranyl Phosphate: Mechanisms and U(IV) Products.
583 *Environmental Science & Technology*, **47**, 5668–5678.

584 RWM. (2015) *Geological Disposal: Introduction to the RWM Waste Package Specification and Guidance*
585 *Documentation*. Didcot, UK, 1–33 pp.

586 RWM. (2016a) *Geological Disposal: Engineered Barrier System status report*. Didcot, UK, 1–146 pp.

RWM. (2016b) *Geological Disposal: Generic Post-closure Safety Assessment*. 1–211 pp.

RWM and NDA. (2015) *Geological Disposal; The 2013 derived inventory*. P. in.: Nuclear Decommissioning Authority 2015, Harwell, Didcot.

Sato, T., Murakami, T., Yanase, N., Hiroshi, I., Payne, T.E. and Airey, P.L. (1997) Iron nodules scavenging uranium from groundwater. *Environmental Science & Technology*, **31**, 2854–2858. American Chemical Society.

Schwertmann, U. and Cornell, R.M. (2000) *Iron oxides in the laboratory: Preparation and characterization*. P. in.: Wiley-VCH Verlag GmbH, Weinheim, Germany, 19–25 pp.

Shelobolina, E.S., Vrionis, H.A., Findlay, R.H. and Lovley, D.R. (2008) Geobacter uraniireducens sp. nov., isolated from subsurface sediment undergoing uranium bioremediation. *International Journal of Systematic and Evolutionary Microbiology*, **58**, 1075–1078. Microbiology Society.

Singh, A., Catalano, J.G., Ulrich, K.-U. and Giammar, D.E. (2012) Molecular-scale structure of uranium(VI) immobilized with goethite and phosphate. *Environmental Science & Technology*, **46**, 6594–6603. American Chemical Society.

Smith, K.F., Bryan, N.D., Swinburne, A.N., Bots, P., Shaw, S., Natrajan, L.S., Mosselmans, J.F.W., Livens, F.R. and Morris, K. (2015) U(VI) behaviour in hyperalkaline calcite systems. *Geochimica et Cosmochimica Acta*, **148**, 343–359.

Suzuki, Y. and Suko, T. (2006) Geomicrobiological factors that control uranium mobility in the environment: Update on recent advances in the bioremediation of uranium-contaminated sites. *Journal of Mineralogical and Petrological Sciences*, **101**, 299–307. Japan Association of Mineralogical Sciences.

Thomas, R.A.P. and Macaskie, L.E. (1996) Biodegradation of tributyl phosphate by naturally occurring microbial isolates and coupling to the removal of uranium from aqueous solution. *Environmental Science and Technology*, **30**, 2371–2375. American Chemical Society .

Thorpe, C.L., Boothman, C., Lloyd, J.R., Law, G.T.W., Bryan, N.D., Atherton, N., Livens, F.R. and Morris, K. (2014) The interactions of strontium and technetium with Fe(II) bearing biominerals: Implications for bioremediation of radioactively contaminated land. *Applied Geochemistry*, **40**, 135–143.

Vali, H., Weiss, B., Li, Y.-L., Sears, S.K., Kim, S.S., Kirschvink, J.L. and Zhang, C.L. (2004) Formation of tabular single-domain magnetite induced by *Geobacter metallireducens GS-15*. *Proceedings of the National Academy of Sciences of the United States of America*, **101**, 16121–6. National Academy of Sciences.

Veeramani, H., Alessi, D.S., Suvorova, E.I., Lezama-Pacheco, J.S., Stubbs, J.E., Sharp, J.O., Dippon, U., Kappler, A., Bargar, J.R. and Bernier-Latmani, R. (2011) Products of abiotic U(VI) reduction by biogenic magnetite and vivianite. *Geochimica et Cosmochimica Acta*, **75**, 2512–2528. Elsevier Ltd.

Vercammen, K., Glaus, M.A., Van Loon, L.R., Ghosh, S., Andersson, P.G., Møller, J., Senning, A., Yao, X.-K., Wang, H.-G., Tuchagues, J.-P. and Ögren, M. (1999) Complexation of calcium by alpha-isosaccharinic acid under alkaline conditions. *Acta Chemica Scandinavica*, **53**, 241–246.

Vettese, G.F., Morris, K., Natrajan, L.S., Shaw, S., Vitova, T., Galanzew, J., Jones, D.L. and Lloyd, J.R. (2020) Multiple Lines of Evidence Identify U(V) as a Key Intermediate during U(VI) Reduction by *Shewanella oneidensis* MR1. *Environmental Science and Technology*, **54**, 2268–2276. American Chemical Society.

Waite, T.D., Davis, J.A., Payne, T.E., Waychunas, G.A. and Xu, N. (1994) Uranium(VI) adsorption to ferrihydrite: Application of a surface complexation model. *Geochimica et Cosmochimica Acta*, **58**, 5465–5478. Pergamon.

Warwick, P., Evans, N., Hall, T. and Vines, S. (2004) Stability constants of uranium(IV)-α-isosaccharinic acid and gluconic acid complexes. *Radiochimica Acta*, **92**, 897–902.

631 Wellman, D.M., Mattigod, S. V., Arey, B.W., Wood, M.I. and Forrester, S.W. (2007) Experimental limitations
632 regarding the formation and characterization of uranium-mineral phases in concrete waste forms. *Cement*
633 *and Concrete Research*, **37**, 151–160.

634 Whistler, R.L. and BeMiller, J.N. (1958) Alkaline degradation of polysaccharides. *Advances in carbohydrate*
635 *chemistry*, **13**, 289–329.

636 Williamson, A.J., Morris, K., Shaw, S., Byrne, J.M., Boothman, C. and Lloyd, J.R. (2013) Microbial reduction
637 of Fe(III) under alkaline conditions relevant to geological disposal. *Applied and Environmental*
638 *Microbiology*, **79**, 3320–3326. American Society for Microbiology.

639 Woolfolk, C.A. and Whiteley, H.R. (1962) Reduction of inorganic compounds with molecular hydrogen by
640 Micrococcus lactilyticus. I. Stoichiometry with compounds of arsenic, selenium, tellurium, transition and
641 other elements. *Journal of Bacteriology*, **84**, 647–658.

642

643